



# CHORUS

This is the accepted manuscript made available via CHORUS. The article has been published as:

## Controlling multimode optomechanical interactions via interference

Mark C. Kuzyk and Hailin Wang

Phys. Rev. A **96**, 023860 — Published 29 August 2017

DOI: [10.1103/PhysRevA.96.023860](https://doi.org/10.1103/PhysRevA.96.023860)

# **Controlling Multimode Optomechanical Interactions via Interference**

Mark C. Kuzyk and Hailin Wang

Department of Physics, University of Oregon, Eugene, OR 97403, USA

## **Abstract**

We demonstrate optomechanical interference in a multimode system, in which an optical mode couples to two mechanical modes. A phase-dependent excitation-coupling approach is developed, which enables the observation of destructive interference in dynamical back-actions. The destructive interference prevents the coupling of the mechanical system to the optical mode, suppressing optically-induced mechanical damping. These studies establish optomechanical interference as an essential tool for controlling the interactions between light and mechanical oscillators.

## I. Introduction

Cavity optomechanics explores fundamental interactions between light and mechanical oscillators[1,2]. While earlier research efforts have focused on simple two-mode systems, in which an optical mode couples only to one mechanical mode, recent efforts have also emphasized multimode systems, in which an optical (or mechanical) mode couples to multiple mechanical (or optical) modes. These multimode systems can provide versatile experimental platforms for a rich variety of physical phenomena, such as exceptional points and topological energy transfer[3], back-action evasion[4,5], two-mode squeezing[6,7], and optical or mechanical state transfers[8-18].

Interference plays a pivotal role in quantum control of multi-level or multi-qubit systems. The advances on multimode systems have thus stimulated strong interest in exploring optomechanical interference processes and in using these processes for applications such as optomechanically-mediated interfaces, entanglement, and ground state cooling[19-24]. For example, when two mechanical modes couple to a common optical mode[3,5-7,13,17,25-27], destructive interference between the respective optomechanical processes can prevent the coupling of the mechanical system to the optical mode, leading to the formation of an optically-dark mechanical superposition mode[23,26]. Similarly, a mechanically-dark optical superposition mode can be formed when two optical modes couple to a common mechanical mode[19,20]. These dark modes can be used for the realization of state transfer as well as two-mode squeezing. The dark optical mode can also be exploited to circumvent the effects of thermal mechanical noise[19,20,22,23]. Evidence for dark optical and dark mechanical modes has been reported in earlier studies[8,26], though there has been no direct experimental probe on the underlying optomechanical interference processes.

In this paper, we report experimental demonstration of optomechanical interference in a multimode system, in which an optical mode couples to two mechanical modes. A phase-dependent excitation-coupling approach is developed for the realization of constructive and destructive interferences. With a phase shift of  $\pi$ , these interference processes can effectively switch the mechanical system from an optically-active to an optically-dark superposition mode. Further experiments on the decay of the dark mode demonstrate directly the suppression of optically-induced mechanical damping and thus the decoupling of the mechanical superposition mode from the optical mode due to the destructive interference in dynamical back-actions. The

interference experiments have been carried out at room temperature and above the thermal background. They can also be extended to the quantum regime. Overall, these studies establish that interference is an effective tool for controlling the interactions between light and mechanical oscillators.

For the three-mode system shown in Fig. 1, two mechanical modes with frequencies  $\omega_{m1}$  and  $\omega_{m2}$  couple to an optical mode with frequency  $\omega_s$ , with the optomechanical coupling driven by two strong external laser fields,  $E_1$  and  $E_2$ , which are respectively  $\omega_{m1}$  and  $\omega_{m2}$  below the optical resonance. The interaction Hamiltonian including only resonant processes is given by

$$V_R = \hbar \hat{a}^\dagger (e^{i\phi_1} G_1 \hat{b}_1 + e^{i\phi_2} G_2 \hat{b}_2) e^{i(\omega_s - \omega_0)t} + h.c. \quad (1)$$

where  $\hat{b}_1$  and  $\hat{b}_2$  are the mechanical annihilation operators in their respective rotating frames,  $\hat{a}$  is the annihilation operator for the optical mode in the rotating frame of a signal field with frequency  $\omega_s$ ,  $\phi_1$  and  $\phi_2$  are the initial phases of  $E_1$  and  $E_2$ , and  $G_1$  and  $G_2$  are the optomechanical coupling rates for the individual mechanical modes. Under these conditions, the mechanical system features bright and dark mechanical modes, described respectively by their annihilation operators,

$$\hat{b}_B = (e^{i\phi_1} G_1 \hat{b}_1 + e^{i\phi_2} G_2 \hat{b}_2) / \sqrt{G_1^2 + G_2^2}, \quad (2a)$$

$$\hat{b}_D = (e^{-i\phi_2} G_2 \hat{b}_1 - e^{-i\phi_1} G_1 \hat{b}_2) / \sqrt{G_1^2 + G_2^2}. \quad (2b)$$

With  $G_1=G_2$ , the two superposition modes in Eq. 2 are completely controlled by the relative optical phase,  $\Delta\phi = \phi_2 - \phi_1$ . In particular, by making a  $\pi$  phase shift in  $\Delta\phi$ , we can turn a bright mechanical mode into a dark mechanical mode.

## II. Experimental setup

A silica microsphere with a diameter near 200  $\mu\text{m}$  is used as a model multimode system. For our experiments, two mechanical whispering gallery (WG) modes, with frequencies  $\omega_{m1}/2\pi=69.48$  MHz and  $\omega_{m2}/2\pi=69.66$  MHz and damping rates  $\gamma_1/2\pi=3.5$  kHz and  $\gamma_2/2\pi=3.6$  kHz, are coupled to a WG optical resonance with a wavelength near 1.55  $\mu\text{m}$  and with damping rate  $\kappa/2\pi=1.6$  MHz. The optomechanical interactions take place via anti-Stokes Brillouin scattering of the optical driving fields from the mechanical modes[28-30]. The input optical

power used for the weak signal field near the optical resonance is less than 0.01 mW. For the optical driving fields, the input optical powers used range from 0.6 to 1.2 mW.

Figure 2 shows the experimental setup. The two optical driving fields,  $E_1$  and  $E_2$ , are derived from a Newport velocity tunable diode laser with a wavelength near 1.55  $\mu\text{m}$ . Two acoustic optical modulators (AOMs) are used to set the relative frequency and phase of the two driving fields. The weak signal field,  $E_s$ , is generated with an electro-optic modulator (EOM) from the driving field  $E_1$ . Two RF signal generators (RF 1a and RF 1b) are used to drive the AOM that generates  $E_1$ . The outputs from RF 1a and RF 1b are first gated and then combined to generate a RF field with a phase slip at specified times. All RF generators except for RF 1b have their external references connected to the same 10 MHz clock (“master clock”). A second 10 MHz signal generator is also locked to the master and sends a reference signal to the RF 1b. We vary the phase of the second 10 MHz generator to generate a phase slip in  $E_1$ .

Optical fields are coupled into and out of whispering gallery optical modes of the silica microsphere via a tapered optical fiber and then detected together in a silicon photodiode, whose output is sent to a real-time spectrum analyzer (SA). This detection scheme can be viewed as heterodyne detection of the emissions from the optical mode, with the two optical driving fields serving as the local oscillators. A relatively small spectral detection window (100 kHz) is used for the SA such that only a single beat frequency is measured in transient measurements. The spectral detection window limits the time-resolution of the experiments to 6  $\mu\text{s}$ .

### III. Experimental results

We have developed a phase-dependent excitation-coupling approach to probe optomechanical interactions and especially interference processes. We first illustrate this approach using a two-mode system. As shown in the inset of Fig. 3, a weak optical signal field,  $E_s$ , with frequency  $\omega_s = \omega_0$ , and an optical driving field,  $E_1$ , with frequency  $\omega_1 = \omega_s - \omega_{m1}$ , couple to the mechanical mode, converting the signal field in the optical mode to a mechanical excitation[31-33]. After  $E_s$  is switched off,  $E_1$  couples to the induced mechanical excitation, converting the mechanical excitation back to optical fields. We introduce a phase slip in  $E_1$  right after  $E_s$  is switched off. The initial phase of  $E_1$  in the excitation stage is  $\theta_1$ . The phase is then changed to  $\phi_1$  in the coupling stage (see Fig. 3).

Heterodyne-detected emissions from the optical mode, with  $E_1$  as the local oscillator, are plotted in Fig. 3 as a function of time. The exponential decay of the emission following the leading edge of the signal pulse corresponds to the increasing conversion of the signal field in the optical mode into the mechanical excitation. The decay time, which sets the timescale for the excitation to reach steady state, is given by  $1/[(1+C_1)\gamma_1]$ , where  $C_1 = 4G_1^2/\gamma_1\kappa = 1.6$  is the cooperativity for the optomechanical coupling. The decrease in the emission from the optical mode in the steady state shown in Fig. 3 corresponds to the dip in the spectral domain optomechanically-induced transparency (OMIT) experiment[33]. The exponential decay after  $E_s$  is switched off corresponds to the conversion of the induced mechanical excitation back into optical fields. With  $\kappa \gg (\gamma_1, G_1)$ , the dynamical back-action underlying this conversion process leads to optically-induced damping of the mechanical excitation[1], with the total damping rate given by  $(1+C_1)\gamma_1$ , as confirmed in Fig. 3. Note that interference also plays an important role in two-mode systems through OMIT[34]. However, the underlying optomechanical coupling cannot be controlled via a phase shift in the optical or mechanical excitations. The experimental result for the two-mode system shown in Fig. 3 is independent of  $\theta_1$  as well as the phase slip  $\phi_1 - \theta_1$ .

We now extend this approach to the three-mode system, for which two optical driving fields,  $E_1$  and  $E_2$ , with frequencies  $\omega_1 = \omega_s - \omega_{m1}$  and  $\omega_2 = \omega_s - \omega_{m2}$ , couple the two mechanical modes to the same optical mode. The pulse sequence of the experiment is shown in Fig. 4a. For simplicity, no phase slip is introduced for  $E_2$ , (i.e.,  $\theta_2 = \phi_2$ ). In the coupling stage, the induced mechanical excitation is in a bright mechanical mode when  $\phi_1 = \theta_1$ . The same excitation, however, is expected to be in a dark mechanical mode when  $G_1 = G_2$  and  $\theta_1$  is  $\pi$  out of phase with  $\phi_1$ . In general, the mechanical excitation can be a combination of both bright and dark modes.

Heterodyne-detected emissions from the optical mode are shown in Figs. 4b and 4c as a function of time. A spectral filter is used such that only the heterodyne beat at frequency  $\omega_{m1}$ , with either  $E_1$  or  $E_2$  as the local oscillator, is detected. The emissions in Figure 4b are detected during the excitation stage of the experiment. Similar to Fig. 3, the decay of the emission in Fig. 4b corresponds to the increasing conversion of the signal field in the optical mode into the mechanical excitations and shows an effective cooperativity of  $C = 1.4$ . The emissions in Fig. 4c are obtained when  $E_s$  is switched off. In this case, the optical driving fields convert the

mechanical excitations back to optical fields, leading to optically-induced mechanical damping. As revealed in Fig. 4c, the optomechanical coupling process depends strongly on the phase slip  $\phi_1 - \theta_1$ .

The heterodyne-detected optical emission energy obtained in a time span of 0.4 ms after  $E_s$  is switched off is plotted in Fig. 4d as a function of  $\phi_1$ . These data are derived from experiments similar to those in Fig. 4c. The interference fringes observed in Fig. 4d are sinusoidal with a period of  $2\pi$ . The minima and maxima in the oscillations correspond respectively to the dark and bright mechanical modes. The sinusoidal oscillations correspond to the switching of the mechanical system between the dark and bright modes as  $\phi_1$  is varied. Similar oscillations are also observed when the heterodyne beat at frequency  $\omega_{m2}$  is detected.

The optomechanical interference underlying the oscillations shown in Fig. 4d occurs in a *self-consistent* two-step process. For the first step,  $E_1$  and  $E_2$  scatter from the relevant mechanical excitations, generating induced signal fields in the optical mode. Under the condition of two-photon resonance,  $\omega_1 + \omega_{m1} = \omega_2 + \omega_{m2}$ , the two induced signal fields are at the same frequency. For the second step, the overall induced signal field and the relevant pump field couple to an individual mechanical mode, leading to dynamical back-actions, more specifically optically-induced mechanical damping[1]. Optomechanical interference takes place through the interference of the induced signal fields in the dynamical back-action. Destructive and constructive interferences in the back-action lead respectively to the formation of dark and bright mechanical modes.

The destructive optomechanical interference effectively decouples the mechanical system from the optical mode, suppressing the optically-induced mechanical damping. For a direct demonstration of the destructive interference in the dynamical back-action, we have measured the damping rate of the dark mode. For this experiment, we append a measurement stage to the pulse sequence in Fig. 4a. As shown in Fig. 5a, after keeping the mechanical system in the dark mode for a duration of  $\tau$ , we switch the initial phase of  $E_1$  back to  $\theta_1$ . Correspondingly, the mechanical system is switched back to the bright mode. Heterodyne-detected optical emissions occurring in the measurement stage probes directly the amplitude of the dark mode at the end of the coupling stage. The emission energy obtained for a time span of 0.4 ms in the measurement stage is plotted in Fig. 5b as function of  $\tau$ . Similar to Fig. 4, only the heterodyne beat at

frequency  $\omega_{m1}$  is detected. Note that the damping rate of the bright mechanical mode can be derived from experiments similar to those in Fig. 4c, in which we measure directly the heterodyne-detected optical emission as a function of time after  $E_s$  is switched off.

The damping rate for the dark mechanical mode, derived from Fig. 5b, is  $\gamma_D/2\pi=7.8$  kHz. In comparison, the damping rate for the bright mechanical mode obtained under otherwise the same experimental condition is  $\gamma_B/2\pi=11$  kHz (see the inset of Fig. 5b), corresponding to  $C=2.1$ . The relative reduction in the optically-induced mechanical damping rate due to the destructive interference is  $(\gamma_B - \gamma_D)/(\gamma_B - \bar{\gamma}) = 43\%$ , where  $\bar{\gamma} = (\gamma_1 + \gamma_2)/2$ . The suppression is not complete, in part due to the slightly unequal damping rates of the two mechanical modes, and to a larger part due to optomechanical coupling processes that are not two-photon resonant. These processes include the coupling of  $E_1$  to mechanical mode 2 and the coupling of  $E_2$  to mechanical mode 1. These two processes do not experience destructive interference, leading to effective damping of the mechanical modes.

### III. Theoretical analysis

For a theoretical analysis of the experimental results, we have used the semi-classical coupled-oscillator equations, with the equations of motion given by

$$\dot{\beta}_1 = -(\gamma_1/2)\beta_1 - ie^{-i\delta t - i\phi_1} G_1 \alpha \quad (3a)$$

$$\dot{\beta}_2 = -(\gamma_2/2)\beta_2 - ie^{-i\delta t - i\phi_2} G_2 \alpha \quad (3b)$$

$$\dot{\alpha} = -(i\Delta + \kappa/2)\alpha - i(e^{i\phi_1} G_1 \beta_1 + e^{i\phi_2} G_2 \beta_2)e^{i\delta t} + \sqrt{\kappa^{ext}} A_s \quad (3c)$$

where  $\beta_1 = \langle \hat{b}_1 \rangle$ ,  $\beta_2 = \langle \hat{b}_2 \rangle$ ,  $\alpha = \langle \hat{a} \rangle$ ,  $\Delta = \omega_0 - \omega_s$ , and  $\kappa^{ext}$  is the cavity decay rate due to input-output coupling. The amplitude of the input signal field,  $A_s$ , is normalized such that  $I_s = |A_s|^2$  is the photon flux. For simplicity, the above equations have assumed that the two-photon resonant condition is satisfied, with  $\delta = \omega_s - \omega_1 - \omega_{m1} = \omega_s - \omega_2 - \omega_{m1}$ , and have omitted coupling terms that are not two-photon resonant (the general equations are given in the appendix). It is straight forward to show from Eq. 3 that with  $\gamma_1 = \gamma_2$ , the amplitude of the dark mode,  $\beta_D = \langle \hat{b}_D \rangle$ , is completely decoupled from the field in the optical mode.

Theoretical calculations, which include both two-photon resonant and non-resonant optomechanical couplings and use experimentally determined parameters, are in good agreement with the experimental results on the fringe visibility shown in Fig. 4d and on the damping rate of the dark mode shown in Fig. 5b. As shown in Fig. 5b, the theoretical calculation that includes only two-photon resonant optomechanical coupling yields a damping rate for the dark mode,  $\gamma/2\pi=3.6$  kHz, nearly the same as  $\gamma_1/2\pi$  and  $\gamma_2/2\pi$ . In this regard, the residual optically-induced mechanical damping for the dark mode is almost entirely due to the two-photon non-resonant couplings, which can be suppressed if the frequency separation between the two mechanical modes far exceed the optical linewidth.

#### **IV. Conclusion**

In conclusion, we have successfully exploited optomechanical interference processes to control optomechanical interactions, in particular, dynamical back-actions, in multimode optomechanical systems. Like its counterpart in multi-level or multi-qubit systems, optomechanical interferences will play an essential role in the exploration and application of interactions between light and mechanical systems.

#### **Acknowledgements**

This work is supported by the National Science Foundation under grant No. 1606227.

## Appendix: Theoretical analysis

We consider the optomechanical coupling between two mechanical modes with frequencies  $\omega_{m1}$  and  $\omega_{m2}$ , and one optical mode with frequency  $\omega_0$ , driven by two strong external laser fields,  $E_1$  and  $E_2$ , which are nearly  $\omega_{m1}$  and  $\omega_{m2}$  below the optical resonance, respectively. In the resolved-sideband limit, the linearized optomechanical Hamiltonian that can satisfy the two-photon resonance condition,  $\omega_2 + \omega_{m2} = \omega_{m1} + \omega_1$ , is given by

$$H_R = \hbar\Delta\hat{a}^\dagger\hat{a} + [\hbar G_1 e^{i(\omega_3 - \omega_1 - \omega_{m1})t + i\phi_1} \hat{a}^\dagger \hat{b}_1 + h.c.] + [\hbar G_2 e^{i(\omega_3 - \omega_2 - \omega_{m2})t + i\phi_2} \hat{a}^\dagger \hat{b}_2 + h.c.] \quad (\text{A1})$$

where  $\hat{b}_1$  and  $\hat{b}_2$  are the annihilation operators for the mechanical modes in their respective rotating frames,  $\hat{a}$  is the annihilation operator for the optical mode in the rotating frame of the signal field with  $\Delta = \omega_0 - \omega_s$ ,  $\phi_1$  and  $\phi_2$  are the initial phase for  $E_1$  and  $E_2$ , and  $G_1$  and  $G_2$  are the effective optomechanical coupling rates for  $E_1$  coupling to mechanical mode 1 and  $E_2$  coupling to mechanical mode 2, respectively. The above Hamiltonian does not contain optomechanical coupling terms that cannot satisfy the two-photon resonant condition. These terms are given by

$$V_{NR} = [\hbar G_{12} e^{i(\omega_3 - \omega_1 - \omega_{m2})t + i\phi_1} \hat{a}^\dagger \hat{b}_2 + h.c.] + [\hbar G_{21} e^{i(\omega_3 - \omega_2 - \omega_{m1})t + i\phi_2} \hat{a}^\dagger \hat{b}_1 + h.c.] \quad (\text{A2})$$

where  $G_{12}$  and  $G_{21}$  are the effective optomechanical coupling rates for  $E_1$  coupling to mechanical mode 2 and  $E_2$  coupling to mechanical mode 1. Note that the non-resonant coupling terms become negligible if the frequency separation between the two mechanical modes far exceeds the optical cavity linewidth.

The semi-classical equations of motion including both two-photon resonant and non-resonant optomechanical interactions are given by

$$\dot{\beta}_1 = -\frac{\gamma_1}{2} \beta_1 - i[G_1 e^{-i(\omega_3 - \omega_1 - \omega_{m1})t - i\phi_1} + G_{21} e^{-i(\omega_3 - \omega_2 - \omega_{m1})t - i\phi_2}] \alpha \quad (\text{A3a})$$

$$\dot{\beta}_2 = -\frac{\gamma_2}{2} \beta_2 - i[G_2 e^{-i(\omega_3 - \omega_2 - \omega_{m2})t - i\phi_2} + G_{12} e^{-i(\omega_3 - \omega_1 - \omega_{m2})t - i\phi_1}] \alpha \quad (\text{A3b})$$

$$\dot{\alpha} = -(i\Delta + \frac{\kappa}{2})\alpha - ie^{i(\omega_3 - \omega_{m1})t} [G_1 e^{i(\phi_1 - \omega_1 t)} + G_{21} e^{i(\phi_2 - \omega_2 t)}] \beta_1 - ie^{i(\omega_3 - \omega_{m2})t} [G_2 e^{i(\phi_2 - \omega_2 t)} + G_{12} e^{i(\phi_1 - \omega_1 t)}] \beta_2 + \sqrt{\kappa} e^{i\omega_s t} A_s \quad (\text{A3c})$$

For a qualitative discussion, we note that the four optomechanical coupling terms in Eq. A3c generate optical fields at frequencies of  $\omega_1 + \omega_{m1}$ ,  $\omega_2 + \omega_{m2}$ ,  $\omega_1 + \omega_{m2}$ , and  $\omega_2 + \omega_{m1}$  through anti-Stokes scattering. Only the two processes corresponding to  $\omega_1 + \omega_{m1}$  and  $\omega_2 + \omega_{m2}$  can satisfy the two-photon resonant condition. All four processes contribute to the optically-induced mechanical damping. For the interference experiments shown in Fig. 4, only the beat frequency at  $\omega_{m1}$  is measured in the heterodyne detection, with either  $E_1$  or  $E_2$  serving as the local oscillator. Under the two-photon resonant condition, optical fields generated by the optomechanical coupling at frequencies,  $\omega_1 + \omega_{m1}$ ,  $\omega_2 + \omega_{m2}$ , and  $\omega_2 + \omega_{m1}$ , contribute to the experiments. The field at  $\omega_1 + \omega_{m2}$  does not contribute to the experiments in Fig. 4.

For the theoretical calculations shown in Figs. 4 and 5, we have solved Eq. A3 numerically using the experimentally determined parameters. To determine the relative contribution of two-photon non-resonant processes to residual optically-induced mechanical damping of the dark mechanical mode, we have also calculated the dark mode decay including only contributions that are two-photon resonant.

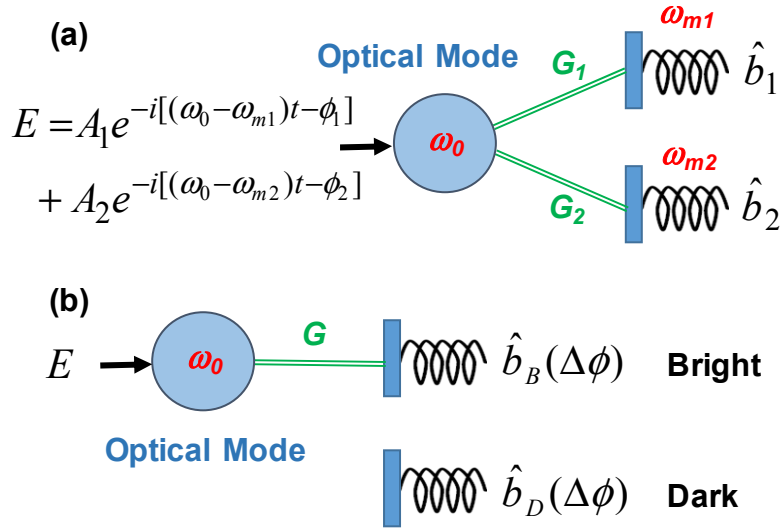


**Figure 1** (a) Schematic of a multimode optomechanical system driven by two optical fields via respective red sideband couplings. (b) Interference between the two optomechanical coupling processes leads to the formation of dark and bright mechanical modes that depend on the relative phase of the optical driving fields,  $\Delta\phi = \phi_2 - \phi_1$ , with the dark mode decoupled from the optical mode.

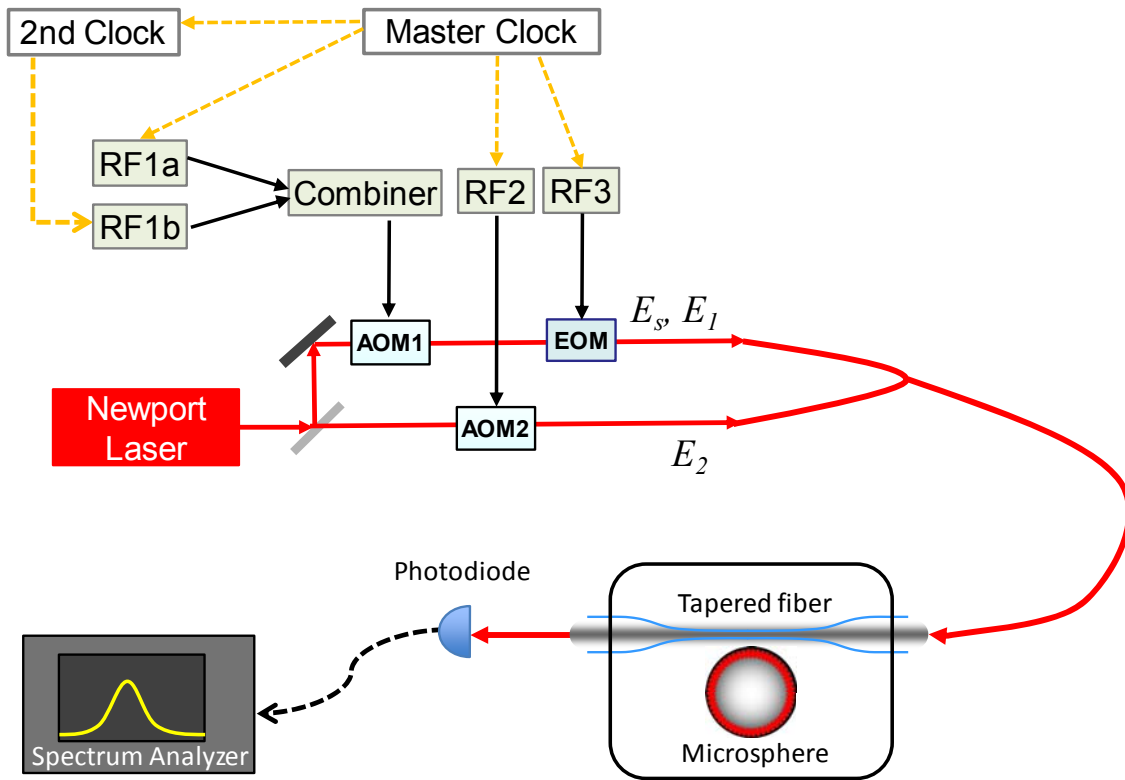


**Figure 2** Schematic of the experimental setup. Optical fields are coupled into and out the relevant whispering gallery optical modes in the microsphere through a tapered fiber.

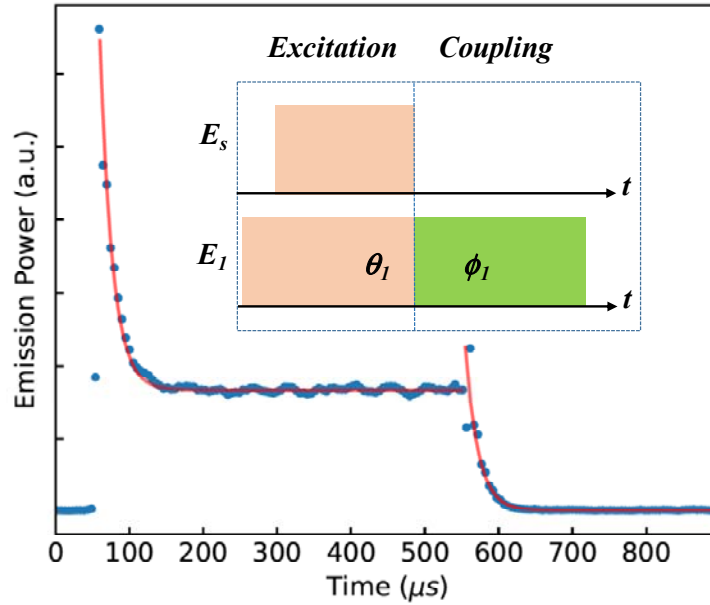


**Figure 3** Heterodyne-detected emissions (the dots) from the optical mode as a function of time in the two-mode system. Solid lines are numerical fits to single exponential decays with a decay rate,  $\gamma/2\pi=9.1$  kHz. The first decay corresponds to the increasing conversion of  $E_s$  to a mechanical excitation. The second decay corresponds to the conversion of the mechanical excitation to optical fields and the resulting mechanical damping, after  $E_s$  is switched off. The inset shows the optical pulse sequence used, with  $E_s$  (0.5 ms in duration) at  $\omega_0$  and  $E_1$  at the red sideband of  $E_s$ .

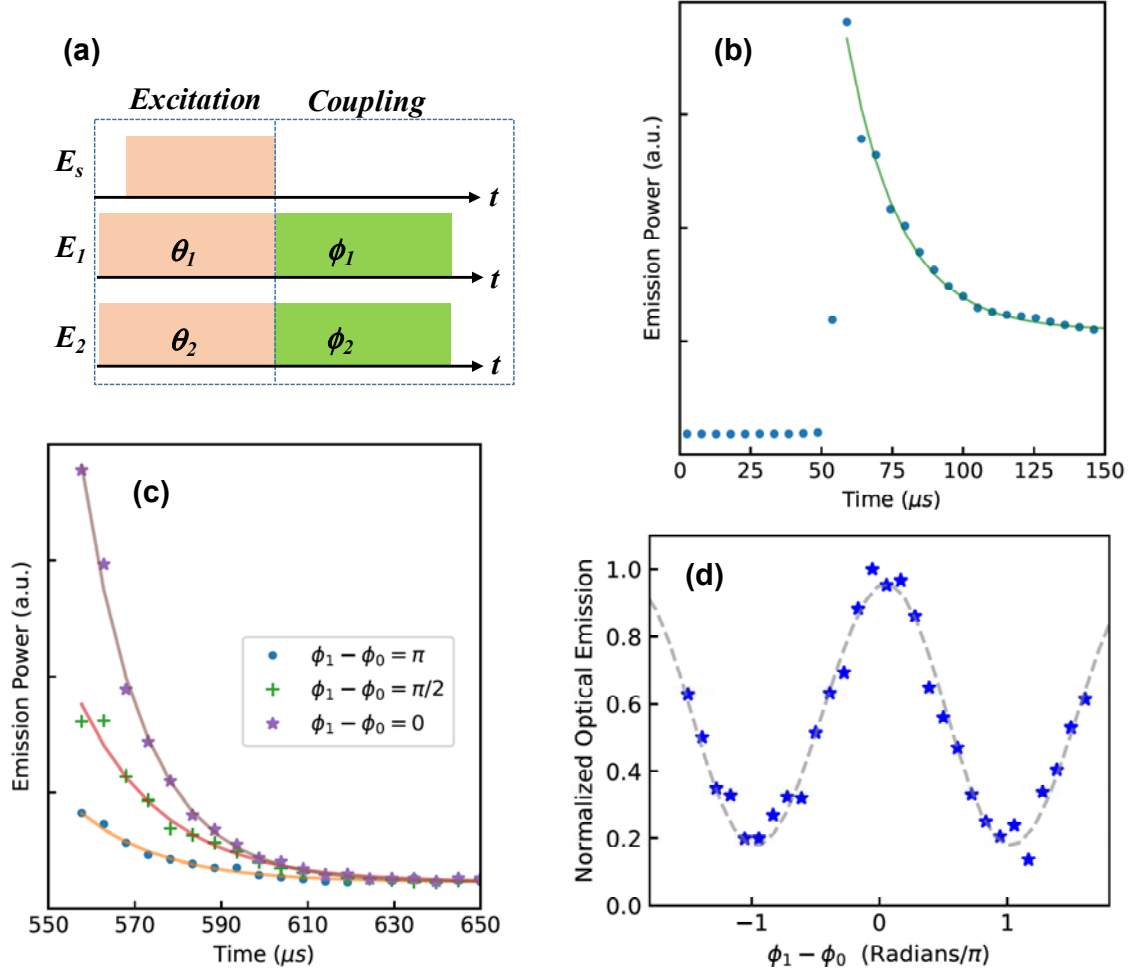


**Figure 4** (a) Optical pulse sequence used for optomechanical interference, with  $E_s$  (0.5 ms in duration) at  $\omega_0$  and  $E_1$  and  $E_2$  at the respective red sidebands of  $E_s$ . (b) Heterodyne-detected emissions from the optical mode as a function of time with  $\theta_2=\phi_2$ , when  $E_s$  is on. (c) Heterodyne-detected emissions from the optical mode as a function of time at various  $\phi_1$  with  $\theta_2=\phi_2$ ,  $C_1=1.3$ , and  $C_2=1$ , when  $E_s$  is off. Solid lines in (b) and (c) are numerical fits to single exponential decays. (d) The emission energy from the optical mode as a function of  $\phi_1$ , obtained in a time span of 0.4 ms after  $E_s$  is switched off. The dashed line shows the theoretical calculation discussed in the text.  $\phi_0$  is an offset such that the dark mode occurs when  $\phi_1-\phi_0=\pi$ .

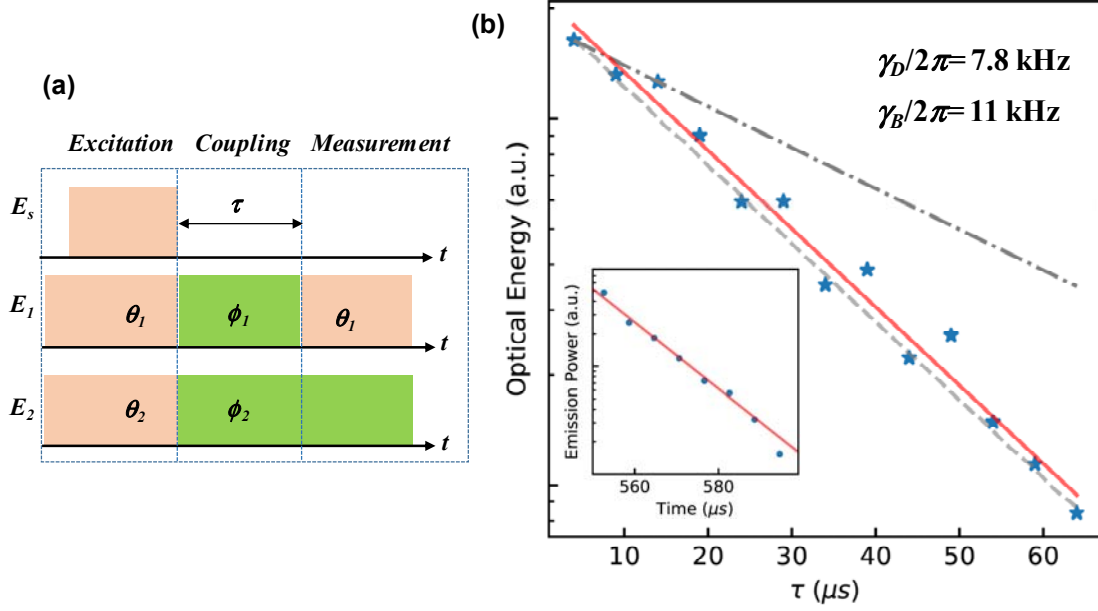


**Figure 5** (a) Optical pulse sequence used to probe the suppression of optically-induced mechanical damping due to destructive interference. (b) Heterodyne-detected optical emissions (the stars) from the optical mode obtained in the measurement stage as a function of  $\tau$ , with  $\theta_2=\phi_2$  and  $G_1= G_2$  and with  $\phi_1$  adjusted such that the mechanical system is in the dark mode in the coupling stage. The dashed line shows the corresponding theoretical calculation discussed in the text. The dash-dotted line shows the theoretical calculation that includes only two-photon resonant optomechanical coupling, yielding a damping rate,  $\gamma/2\pi=3.6$  kHz. The inset shows the measurement of the bright mode decay in the coupling stage. The solid lines are numerical fits of the experimental data to single exponential decays.

## References:

- [1] M. Aspelmeyer, T. J. Kippenberg, and F. Marquard, *Cavity optomechanics*, *Reviews of Modern Physics* **86**, 1391 (2014).
- [2] M. Aspelmeyer, P. Meystre, and K. Schwab, *Quantum optomechanics*, *Physics Today* **65(7)**, 29 (2012).
- [3] H. Xu, D. Mason, L. Y. Jiang, and J. G. E. Harris, *Topological energy transfer in an optomechanical system with exceptional points*, *Nature* **537**, 80 (2016).
- [4] J. B. Hertzberg, T. Rocheleau, T. Ndukum, M. Savva, A. A. Clerk, and K. C. Schwab, *Back-action-evading measurements of nanomechanical motion*, *Nature Physics* **6**, 213 (2010).
- [5] C. F. Ockeloen-Korppi, E. Damskagg, J. M. Pirkkalainen, A. A. Clerk, M. J. Woolley, and M. A. Sillanpaa, *Quantum Backaction Evading Measurement of Collective Mechanical Modes*, *Physical Review Letters* **117**, 140401 (2016).
- [6] C. H. Dong, J. T. Zhang, V. Fiore, and H. L. Wang, *Optomechanically induced transparency and self-induced oscillations with Bogoliubov mechanical modes*, *Optica* **1**, 425 (2014).
- [7] A. Pontin, M. Bonaldi, A. Borrielli, L. Marconi, F. Marino, G. Pandraud, G. A. Prodi, P. M. Sarro, E. Serra, and F. Marin, *Dynamical Two-Mode Squeezing of Thermal Fluctuations in a Cavity Optomechanical System*, *Physical Review Letters* **116**, 103601 (2016).
- [8] C. Dong, V. Fiore, M. C. Kuzyk, and H. Wang, *Optomechanical dark mode*, *Science* **338**, 1609 (2012).
- [9] J. T. Hill, A. H. Safavi-Naeini, J. Chan, and O. Painter, *Coherent optical wavelength conversion via cavity optomechanics*, *Nature Communications* **3**, 1196 (2012).
- [10] Y. Liu, M. Davanço, V. Aksyuk, and K. Srinivasan, *Electromagnetically induced transparency and wideband wavelength conversion in silicon nitride microdisk optomechanical resonators*, *Physical Review Letters* **110**, 223603 (2013).
- [11] J. Bochmann, A. Vainsencher, D. D. Awschalom, and A. N. Cleland, *Nanomechanical coupling between microwave and optical photons*, *Nature Physics* **9**, 712 (2013).
- [12] R. W. Andrews, R. W. Peterson, T. P. Purdy, K. Cicak, R. W. Simmonds, C. A. Regal, and K. W. Lehnert, *Bidirectional and efficient conversion between microwave and optical light*, *Nature Physics* **10**, 321 (2014).
- [13] A. B. Shkarin, N. E. Flowers-Jacobs, S. W. Hoch, A. D. Kashkanova, C. Deutsch, J. Reichel, and J. G. E. Harris, *Optically Mediated Hybridization between Two Mechanical Modes*, *Physical Review Letters* **112**, 013602 (2014).
- [14] R. W. Andrews, A. P. Reed, K. Cicak, J. D. Teufel, and K. W. Lehnert, *Quantum-enabled temporal and spectral mode conversion of microwave signals*, *Nature Communications* **6**, 10021 (2015).
- [15] F. Lecocq, J. B. Clark, R. W. Simmonds, J. Aumentado, and J. D. Teufel, *Mechanically Mediated Microwave Frequency Conversion in the Quantum Regime*, *Physical Review Letters* **116**, 043601 (2016).
- [16] K. C. Balram, M. I. Davanco, J. D. Song, and K. Srinivasan, *Coherent coupling between radiofrequency, optical and acoustic waves in piezo-optomechanical circuits*, *Nature Photonics* **10**, 346 (2016).
- [17] M. J. Weaver, F. M. Buters, F. Luna, H. J. Eerkens, K. Heck, S. de Man, and D. Bouwmeester, *Coherent Optomechanical State Transfer between Disparate Mechanical Resonators*, arXiv:1701.04212 (2017).

- [18] C. H. Dong, Y. D. Wang, and H. L. Wang, *Optomechanical interfaces for hybrid quantum networks*, Natl Sci Rev **2**, 510 (2015).
- [19] Y. D. Wang and A. A. Clerk, *Using Interference for High Fidelity Quantum State Transfer in Optomechanics*, Physical Review Letters **108**, 153603 (2012).
- [20] L. Tian, *Adiabatic State Conversion and Pulse Transmission in Optomechanical Systems*, Physical Review Letters **108**, 153604 (2012).
- [21] H. Seok, L. F. Buchmann, E. M. Wright, and P. Meystre, *Multimode strong-coupling quantum optomechanics*, Physical Review A **88**, 063850 (2013).
- [22] L. Tian, *Robust Photon Entanglement via Quantum Interference in Optomechanical Interfaces*, Physical Review Letters **110** (2013).
- [23] Y. D. Wang and A. A. Clerk, *Reservoir-Engineered Entanglement in Optomechanical Systems*, Physical Review Letters **110**, 253601 (2013).
- [24] Y. Yanay, J. C. Sankey, and A. A. Clerk, *Quantum backaction and noise interference in asymmetric two-cavity optomechanical systems*, Physical Review A **93**, 063809 (2016).
- [25] Q. Lin, J. Rosenberg, D. Chang, R. Camacho, M. Eichenfield, K. J. Vahala, and O. Painter, *Coherent mixing of mechanical excitations in nano-optomechanical structures*, Nature Photonics **4**, 236 (2010).
- [26] F. Massel, S. U. Cho, J. M. Pirkkalainen, P. J. Hakonen, T. T. Heikkilä, and M. A. Sillanpää, *Multimode circuit optomechanics near the quantum limit*, Nature Communications **3**, 987 (2012).
- [27] N. Spethmann, J. Kohler, S. Schreppler, L. Buchmann, and D. M. Stamper-Kurn, *Cavity-mediated coupling of mechanical oscillators limited by quantum back-action*, Nature Physics **12**, 27 (2016).
- [28] G. Bahl, M. Tomes, F. Marquardt, and T. Carmon, *Observation of spontaneous Brillouin cooling*, Nature Physics **8**, 203 (2012).
- [29] J. Kim, M. C. Kuzyk, K. W. Han, H. L. Wang, and G. Bahl, *Non-reciprocal Brillouin scattering induced transparency*, Nature Physics **11**, 275 (2015).
- [30] C. H. Dong, Z. Shen, C. L. Zou, Y. L. Zhang, W. Fu, and G. C. Guo, *Brillouin-scattering-induced transparency and non-reciprocal light storage*, Nature Communications **6**, 6193 (2015).
- [31] J. Zhang, K. Peng, and S. L. Braunstein, *Quantum-state transfer from light to macroscopic oscillators*, Physical Review A **68**, 013808 (2003).
- [32] V. Fiore, Y. Yang, M. C. Kuzyk, R. Barbour, L. Tian, and H. Wang, *Storing optical information as a mechanical excitation in a silica optomechanical resonator*, Physical Review Letters **107**, 133601 (2011).
- [33] C. H. Dong, V. Fiore, M. C. Kuzyk, and H. L. Wang, *Transient optomechanically induced transparency in a silica microsphere*, Physical Review A **87**, 055802 (2013).
- [34] G. S. Agarwal and S. M. Huang, *Electromagnetically induced transparency in mechanical effects of light*, Physical Review A **81**, 041803 (2010).